



**University of
Zurich**^{UZH}

**Zurich Open Repository and
Archive**

University of Zurich
University Library
Strickhofstrasse 39
CH-8057 Zurich
www.zora.uzh.ch

Year: 2020

Predifferentiated Smooth Muscle-Like Adipose-Derived Stem Cells for Bladder Engineering

Smolar, Jakub ; Horst, Maya ; Salemi, Souzan ; Eberli, Daniel

DOI: <https://doi.org/10.1089/ten.TEA.2019.0216>

Posted at the Zurich Open Repository and Archive, University of Zurich

ZORA URL: <https://doi.org/10.5167/uzh-187969>

Journal Article

Accepted Version

Originally published at:

Smolar, Jakub; Horst, Maya; Salemi, Souzan; Eberli, Daniel (2020). Predifferentiated Smooth Muscle-Like Adipose-Derived Stem Cells for Bladder Engineering. *Tissue Engineering. Part A*, 26(17-18):979-992.

DOI: <https://doi.org/10.1089/ten.TEA.2019.0216>

Pre-differentiated smooth muscle-like adipose-derived stem cells for bladder engineering

Authors: Jakub Smolar^{1c}, Maya Horst^{2c}, Souzan Salemi¹, Daniel Eberli^{1*}

¹Department of Urology, University Hospital Zurich, Switzerland

²Division of Pediatric Urology, University Children's Hospital Zurich, Switzerland

*Corresponding author

^c Split first author

Keywords: Stem cell, Co-culture, Bladder smooth muscle, Regenerative medicine, Proteome

Jakub Smolar, PhD

jakub.smolar@usz.ch, Tel: +41 255 11 11

Laboratory for Tissue Engineering, University Zurich, Wagistrasse 21, Schlieren ZH, Switzerland

Maya Horst, PD Dr. med.

Maya.Horst@kispi.uzh.ch, Tel: +41 266 71 11

Laboratory for Tissue Engineering, University Zurich, Wagistrasse 21, Schlieren ZH, Switzerland

Souzan Salemi, PhD

Souzan.Salemi@usz.ch, Tel: +41 255 11 11

Laboratory for Tissue Engineering, University Zurich, Wagistrasse 21, Schlieren ZH, Switzerland

This paper has been peer-reviewed and accepted for publication, but has yet to undergo copyediting and proof correction. The final published version may differ from this proof.

Tissue Engineering

Pre-differentiated smooth muscle-like adipose-derived stem cells for bladder engineering (DOI: 10.1089/ten.TEA.2019.0216)

Daniel Eberli (Corresponding Author), Prof. Dr. med. Dr. rer. nat.

daniel.eberli@usz.ch, Tel: +41 255 11 11

Laboratory for Tissue Engineering, University Hospital Zürich, Frauenklinikstrasse 10, 8091
Zürich Switzerland

Abstract

Introduction: All organs of human body are a conglomerate of various cells types with multi-directional interplay between the different cells and the surrounding microenvironment, leading to a stable tissue formation, homeostasis and function. In order to develop a functional smooth muscle tissue, we need to simulate and create a multicellular microenvironment. The multi-lineage adipose-derived stem cells (ADSC), which can be easily harvested in large numbers, may provide an alternative cell source for the replacement of smooth muscle cells (SMC) in cell-based detrusor bioengineering therapeutic approaches. The aim of this study was to investigate whether pre-differentiated smooth muscle-like ADSC (pADSC) can support SMC to generate stable smooth muscle tissue through remodeling of ECM and factor secretion.

Methods: Rat SMC and pADSC were mono- and co-cultured in the cell ratios 1:1, 1:2, 1:3 and 1:5 (SMC-pADSC) and grown for up to two weeks *in vitro*. The expression of the SMC-specific markers alpha smooth muscle actin (α SMA), calponin, myosin heavy chain 11 (MyH11) and smoothelin was assessed and cell proliferation and contractility analyzed. Proteomic analysis of the secretome (cell-cell contact were compared to a non-contact transwell 1:1 co-culture) and the cell pellets was performed, with the focus on ECM deposition and remodeling, integrin expression and growth factor secretion.

Results: SMC and pADSC were strongly positive for all smooth muscle markers. After one and two weeks of culture, the 1:1 cell ratio developed a significantly higher number of smooth muscle organoids and improved contractility. These organoids were highly structured, consisting of an SMC core surrounded by a pADSC layer. The deposition of various EMC proteins, such as collagens 1a1, 1a2, 2a1, 3a1, 5a2, 6a2, 12a1 and fibrillin 1 was significantly increased. A decreased MMP3, MMP9 and MMP13 secretion, as well as an increased TIMP1 and TIMP2 secretion were found in the contact co-culture compared to the monoculture controls.

Conclusion: SMC-pADSC 1:1 co-cultures exhibits an improved cell proliferation, contractility and organoid formation compared to all other ratios and monoculture, while retaining a stable phenotype that is comparable to the SMC monoculture. These effects

are mediated by increased ECM deposition and tight ECM remodeling by the secreted MMP and TIMP.

Impact Statement

Harvesting smooth muscle cells from diseased bladders represents a significant limitation for clinical translation of bladder Tissue Engineering. Our results suggest that autologous pADSC can substitute SMCs, and may be used in combination with SMC to generate contractile detrusor muscle tissue for patients suffering from end-stage bladder diseases. We demonstrate a beneficial effect when using these cells in a 1:1 ratio with improved deposition of ECM molecules and superior remodeling of the ECM by MMPs and decreased TIMP activity.

Introduction

The urinary bladder is a complex hollow organ that consists of the urothelium on its luminal side, the underlying lamina propria and a major functional outer layer - the detrusor muscle [1]. In patients suffering from neuropathic bladders and other end-stage bladder diseases, the detrusor muscle often is denervated and fibrotic, heavily impairing the function and regeneration of the whole organ [2]. Currently, one of the most promising experimental methods to reconstruct and regenerate damaged detrusor muscle is the cell-based bladder augmentation [3] using autologous bladder smooth muscle cells (SMC) isolated from biopsies [4], in combination with a biocompatible scaffold. However, SMC show a restricted proliferative capacity and loss of the contractile phenotype [5] *in vitro*. Furthermore, healthy autologous SMC are often limited in diseased bladder tissue [6,7]. Substituting a significant percentage of contractile cells needed for bladder tissue engineering by pre-differentiated autologous adipose-derived stem cells (pADSC) would reduce the bottleneck for clinical translation. This strategy would require a smaller biopsy of smooth muscle tissue with less morbidity, less chances of adverse phenotype passed down from the diseased organ and overcome the growth limitations of SMCs.

ADSC are highly abundant in human adipose tissue and can be comparatively easily isolated using minimally invasive techniques[8] and grown under standard culture conditions[9] while maintaining an undifferentiated, highly proliferative phenotype for extended periods *in vitro* [10]. Moreover, ADSC were shown to differentiate along multiple lineages of all three germ lines and generate adipocytes, chondrocytes, myocytes and osteoblasts[9], as well as hepatocytes [11], epithelial [12], neural [13] and vascular tissues [14]. In addition, ADSC display angiogenic [15], antifibrotic [16] and immunomodulatory properties[17]. The incubation of ADSC in smooth muscle differentiation media, resulted in the upregulation of α -smooth muscle actin (SMA), calponin, caldesmon, SM22, myosin heavy chain and smoothelin [18] turning them into smooth muscle-like cells. Another efficient way to obtain large numbers of smooth muscle-like cells from ADSC is by their incubation in MCDB-131 culture media supplemented with heparin [19] or by the addition of TGF- β 1 and bone morphogenic protein (BMP)4 to a standard culture media [20]. More

complex approaches to generate bladder-like SMC may involve a two-step differentiation, such as in the case of rabbit ADSC [21].

The efficiency of undifferentiated ADSC treatment of bladder injury has already been tested in several small animal models. Direct treatment with ADSC has led to an improved bladder architecture [22], while a combined treatment with bladder acellular matrix (BAM) led to an improved smooth muscle formation and neuronal ingrowth [23]. Furthermore, ADSC-seeded BAM resulted in detrusor muscle and neuronal regeneration, and an improved bladder capacity in a rat bladder augmentation model [24].

In our study, ADSC were pre-differentiated into smooth muscle-like cells (pADSC) in order to commit them to a stable smooth muscle lineage. Further, the effect of pADSC on SMCs and vice versa in a contact and non-contact transwell co-culture system was investigated, assessing the cell proliferation, SMC marker expression and contractility between different cell ratios and the respective monoculture controls. In addition, growth factor secretion, ECM deposition and remodeling, and the integrin expression of the best performing SMC–pADSC ratio in a contact co-culture was analyzed using proteomics and compared to controls.

Materials and methods

SMC isolation and culture: SMC were isolated from bladders of female Lewis rats according to established protocols and in accordance with the animal ethics committee guidelines (110/2015). Rat bladders were excised and washed in phosphate-buffered saline (PBS, Invitrogen, Carlsbad USA) containing 1% penicillin/streptomycin (PS, Invitrogen). Adherent blood vessels, adipose tissue and the urothelium were removed. The remaining detrusor muscle was cut into narrow pieces, placed on 10cm CellBind® cell culture dishes (Nunc, Roskilde DNK), and left for 5 minutes to dry. Standard cell culture medium containing DMEM/F12+GlutaMAX (Invitrogen), 10% fetal bovine serum (FBS, Merck, Darmstadt GER) and 1% PS was added.

ADSC isolation and culture: ADSC were isolated from subcutaneous adipose tissue of Lewis rats. The adipose tissue was minced and digested for one hour at 37°C using collagenase type I-S (Merck) and further processed, expanded and purified according to the

established protocols [19,25]. ADSC phenotype and multilineage plasticity were tested in our lab as described by Salemi et al.[19]. All experiments were carried out using ADSC and SMCs between passages 4 and 5.

Differentiation of ADSC into pADSC: ADSC were differentiated using an established protocol[19]. Briefly, undifferentiated ADSC were expanded to 80-90% confluence, replated and incubated for three weeks in SMC-inductive MCDB-131 medium (Merck) supplemented with 1% FBS, 1% PS and 100U/ml heparin (Bichsel, CH). Harvesting of the differentiated cells was performed by trypsinisation.

Cell characterization: Expanded SMC and differentiated pADSC were characterized by indirect immunostaining and flow cytometry using SMC specific markers calponin [1:100] (Merck), myosin heavy chain (MyH)11 [1:5] and smoothelin [1:100] (Santa Cruz Biotechnology, Dallas USA).

Co-culture experiments: Cell co-culture ratio of 1:1 (SMC-pADSC), 1:3 and 1:5 were used as starting points for our experiments. During our pursuit to find the best performing and likely the clinically most suitable SMC-pADSC ratio we also included an additional ratio of 1:2 at a later stage of the experiments.

Immunofluorescence staining: Samples were fixed overnight using 4% paraformaldehyde in PBS (Artechemis, CH). Indirect immunostaining on 0.3% Triton X-100 (Merck) permeabilized cells was performed at room temperature for 1.5h. Dako mounting media (Agilent, Santa Clara USA) was used. Cells were analyzed for the expression of all three specific SMC markers calponin, MyH11 and smoothelin at each timepoint using a Leica DMIL LED microscope and Leica LAS X software (Leica Microsystems, Wetzlar GER).

Flow cytometry: pADSC and SMC were trypsinized using a 0.25% Trypsin-EDTA solution (Invitrogen), pelleted, washed with PBS and stained indirectly for calponin, MyH11 and smoothelin using the Foxp3 Buffer Set (Thermo Scientific, Waltham USA) according to manufacturer's protocol. Flow cytometry was performed on BD FACSAria III and analysed by FlowJo X software (FlowJo, Ashland USA).

Organoid growth and size were assessed after one, two and three weeks of culture. Three random pictures were taken per sample in triplicates and number of organoids was determined by manual counting. Organoid size was measured using ImageJ software (NIH, Bethesda USA).

Cell proliferation: SMC and pADSC mono- and co-cultures were cultured in standard culture media for up to eight days. Cell proliferation reagent WST-1 (Merck) was used to measure their proliferation at days one, two, four and eight according to manufacturer's protocol.

In-cell western blot: Cells were seeded in 96-well plates in 1:1, 1:2 and 1:3 co-culture ratios and grown for one and two weeks. SMC were used as a control. No separation of cell types was done for the analysis. At each time point, cells were washed and fixed over night with 4% paraformaldehyde, permeabilized and stained for α SMA, calponin and smoothelin according to manufacturer's protocol. Results were obtained using the LI-COR Odyssey system (LI-COR, Lincoln USA).

Gel contraction assay: Spontaneous contractility was examined [26]. SMC were used as positive and ADSC as negative controls. Cells were embedded in floating collagen type I discs and incubated in standard culture media for up to 48h. Pictures were taken using a digital camera at a fixed distance and the disc areas were calculated using ImageJ software.

PKH cell tracking in 2D and 3D: cells were stained either with PKH26 or PKH67 (Merck) according to manufacturer's protocol. Stained SMC and pADSC were then combined in a 1:1 ratio and grown either on glass chamber slides or embedded in bovine collagen type I (Merck) to assess their interaction in 2D and 3D microenvironments. Pictures were taken after fixation with 4% paraformaldehyde using LEICA DMIL LED microscope and the Cytation 5 imaging system (BioTek, Winooski USA).

Proteomic sample preparation: Co-cultures with cell-cell contact and non-contact transwell SMC-pADSC co-cultures in a 1:1 ratio and the respective monocultures were grown in 6-well plates for two weeks. Cells were washed extensively with PBS and serum-free standard culture medium was added. The supernatant was collected after 24h, cells were

released, washed, pelleted, shock frozen and stored at -80°C until analysis. Proteins from supernatant samples were precipitated with acetone. All samples were resuspended in 8M urea and 0.1M ammonium bicarbonate and tryptic peptides were prepared as described [27].

Proteomic LC-MS/MS analysis - Supernatants: Two sample pools were generated from aliquots of each supernatant sample and High-pH reverse phase chromatography (HPRP) fractionation of each pool was performed using a MicroSpin C18 column (Thermo Scientific). The resulting five fractions were analyzed using an Easy-nLC 1200 (60 min chromatographic gradient) connected to a Fusion Lumos Tribrid mass spectrometer (Thermo Scientific) operating in DDA mode[27]. A modified top speed method (3s cycle time) was used[28]. A sample-specific spectral library was generated by searching DDA data against a rat UniProt protein database (TrEMBL, 2018-01-01) using Pulsar search engine (Biognosys, Schlieren CH) allowing for two missed cleavages and variable modifications (acetylation (protein N-term), oxidation (M), deamidation (NQ) and carbamylation (KR)). DIA LC-MS/MS analysis was performed on the same instrumentation by injecting 2µg of tryptic peptides per sample, using a method with one full range survey scan and 25 DIA windows. DIA data was analyzed using Spectronaut software (Biognosys) with the sample-specific spectral library[27].

Proteomic LC-MS/MS analysis - Cell Pellets: Two sample pools were generated from aliquots of each supernatant sample and HPRP fractionation of each pool was performed using an UHPLC system[27]. The resulting four fractions were analyzed using an Easy-nLC 1200 (120 min chromatographic gradient) connected to a Q Exactive HF mass spectrometer (Thermo Scientific) operating in DDA mode[27]. A modified TOP12 method was used[29]. A sample-specific spectral library was generated by searching DDA data against a rat UniProt protein database (TrEMBL, 2018-01-01) using Pulsar search engine (Biognosys) allowing for two missed cleavages and variable modifications (acetylation (protein N-term), oxidation (M)). DIA LC-MS/MS analysis was performed on the same instrumentation, using a method with one full range survey scan and 22 DIA windows. DIA data was analyzed using Spectronaut software (Biognosys) with the sample-specific spectral library[27].

Statistical analysis: was performed using GraphPad Prism 6.01 (GraphPad Software, La Jolla USA) by unpaired T-tests, ANOVA or two-way ANOVA and Bonferroni's comparison method, depending on the group comparison and sample size. Statistically significant differences were defined as * $P < 0.05$, ** $P < 0.01$, *** $P < 0.001$ and **** $P < 0.0001$. Values in graphs were presented as Median with range, Boxplots \pm Min/Max or Scatter dot plot \pm Min/Max.

Results

Cell characterization after expansion and differentiation: SMC subjected to immunofluorescence staining showed a high expression of all SMC markers calponin, MyH11 and smoothelin. pADSC exhibited a similar expression of calponin and smoothelin, and a decreased expression of MyH11 compared to the SMC. ADSC were negative for all SMC markers (Suppl. Fig. 1a). These results were confirmed by flow cytometry (Suppl. Fig. 1b).

Morphology and phenotype changes in the cell co-cultures over time: Changes in cell morphology and SMC marker expression in the different co-cultures were assessed over two weeks. After one week of culture, SMC showed a strong expression of all three SMC markers calponin, MyH11 and smoothelin. The co-cultures in ratios 1:1 and 1:3 showed a comparable expression of all three markers, while the 1:5 cell ratio exhibited a weaker, rather inconsistent SMC marker expression (Fig. 1 and Supl 1a). At the two-week time point, the 1:1 and 1:3 cell co-cultures showed a similar SMC marker expression to each other and the SMC control, while the cells grown in 1:5 ratio expressed calponin and MyH11 in a weaker manner (Fig. 1, right columns).

The 1:1 cell ratio exhibited a significantly higher average organoid number after one (9.556) and two (13.11) weeks of culture, compared to the 1:3 (3.778, $P^* < 0.001$ and 9.0, *n.s.*), 1:5 (4.222, $P^* < 0.01$ and 7.556, $P^* < 0.001$) cell co-cultures and the SMC monoculture (0, $P^* < 0.0001$ and 4.667, $P^* < 0.0001$) respectively (Fig. 2a). The average organoid size remained constant in all conditions and at both time points (data not shown).

Organoid structure in 2D and 3D systems: In order to assess the importance of paracrine signaling between SMC and pADSC on the organoid formation, both cell types were also

co-cultured under non-contact transwell conditions. Already after one week of 2D culturing, with pADSC above the transwell, SMC began forming organoids, while pADSC did not show any organoid formation, when SMCs were above the transwell during three weeks of culture (Fig. 2b). SMC and pADSC were stained with pkh67 and PKH26 respectively, mixed and co-cultured on glass chamber slides (2D) in a 1:1 ratio for two weeks. Morphological analysis showed that SMC formed the “core” of the organoid, while pADSC grew over and along the SMC (Fig. 2b+c). Similar development was observed with PKH-stained cells grown in collagen scaffolds (3D), where SMC formed the bulk of the organoids, which was surrounded by the pADSC (Suppl. Fig. 2, left column). Moreover, large fiber-like structures of macroscopically visible, interconnected SMC networks developed in the hydrogels with pADSC covering these structures (Suppl. Fig. 2, middle and right columns).

Cell proliferation: Based on our previous observation during the cell co-culture experiments, we performed the cell proliferation analysis for up to eight days using the WST-1 reagent, and included the 1:2 cell ratio. pADSC and SMC proliferated in a similar manner in the first two days of culture. However, after four days of culture pADSC showed a significantly increased proliferation compared to the SMC ($P^* < 0.0001$) that further increased at the eight day time point. Overall, the cell co-cultures in the ratios 1:1, 1:2 and 1:3 proliferated significantly faster than the monocultures ($P^* < 0.0001$). However, the 1:5 cell co-culture proliferated similarly to the pADSC monoculture until day four, exhibiting a significantly lower proliferation at day eight ($P^* < 0.05$). There was a significant increase in proliferation in the 1:1 cell co-culture compared to all other conditions after four days ($P^* < 0.0001$), which then normalized between the 1:1, 1:2 and 1:3 cell co-cultures at day eight (Fig. 3a).

The paracrine effect on their respective proliferation was investigated in a transwell non-contact experiment. There was no significant difference in SMC proliferation between the three SMC-pADSC ratios in the first four days of culture. However, at day eight a significant, ratio-dependent increase in SMC proliferation ($P^* < 0.0001$) was observed (Fig. 3b). The non-contact transwell co-cultured pADSC showed a significantly increased proliferation regardless the cell ratios during the whole experiment ($P^* < 0.0001$). A

significant higher proliferation ($P^* < 0.0001$) was observed in the 1:1 compared to the 1:3 cell ratios at day eight of the co-culture (Fig. 3c).

Quantification of SMC marker expression: The SMC marker expression was quantified using direct in-cell western blot staining of the 1:1, 1:2 and 1:3 cell co-cultures and the SMC control. The 1:5 cell ratio was not included in this analysis anymore, as the previous experiments have shown that this cell co-culture does not perform well enough in terms of phenotype stability, organoid formation and proliferation. In general, the expression of all SMC markers almost doubled between the first and the second week of culture (Fig. 3d). Compared to the SMC control, the α SMA expression was significantly increased in the 1:1 ($P^* < 0.05$) and significantly decreased in both 1:2 and 1:3 cell co-cultures ($P^* < 0.0001$ and $P^* < 0.001$) after one week of culture. After two weeks, the cell co-cultures showed a ratio-dependent, significant decrease of α SMA expression compared to the SMC monoculture ($P^* < 0.0001$), with the 1:1 cell co-culture exhibiting the closest expression level to the control ($P^* < 0.01$). Calponin expression was significantly decreased in the 1:1 ($P^* < 0.05$), the 1:2 and 1:3 ($P^* < 0.0001$) co-cultures compared to the SMC monoculture at the one-week timepoint. There was no significant difference between the 1:2 co-culture and the control after two weeks of culture. In comparison, 1:1 ($P^* < 0.05$) and 1:3 ($P^* < 0.01$) cell co-cultures showed a significantly decreased expression to the SMC monoculture at this timepoint. There was no significant difference between the co-cultures and the SMC control in smoothelin expression after the first week of culture. However, after two weeks, smoothelin expression was significantly decreased in all cell co-cultures compared to the SMC monoculture ($P^* < 0.0001$).

Cell contractility: In order to assess the difference in contractility among the 1:1, 1:2 and 1:3 cell ratios a gel contractility assay was performed (Fig. 4). Overall, the SMC monoculture and all co-cultures showed a significantly increased contractility after 24 ($P^* < 0.001$) and 48h ($P^* < 0.0001$) compared to the ADSC control. The 1:1 cell co-culture contracted comparable to the SMC monoculture over the duration of the whole experiment, while the 1:2 and 1:3 cell co-cultures showed a lower but similar contractility to each other. There was a significant difference in contractility between the SMC/1:1 and the 1:2/1:3 groups ($P^* < 0.01$) after 24h, which disappeared at the 48h time point.

Proteomic analysis: Based on our results, the 1:1 cell co-culture with cell-cell contact was chosen for the proteomic secretome and cell pellet analysis and compared to the non-contact transwell co- and the respective monocultures.

Proteomic analysis – ECM deposition: A variety of ECM proteins important in cell niche generation were found in the secretome of all samples (Fig. 5). Collagen (Col)1a1 was secreted significantly higher by the contact than the non-contact transwell co-culture ($P^* < 0.01$) and the SMC monoculture ($P^* < 0.001$). Collagens 1a2 ($P^* < 0.001$), Col2a1 ($P^* < 0.05$, $P^* < 0.001$, $P^* < 0.0001$), Col3a1 ($P^* < 0.0001$), Col5a2 ($P^* < 0.01$), Col6a2 ($P^* < 0.01$, $P^* < 0.001$, $P^* < 0.0001$) and fibrillin1 ($P^* < 0.01$) were secreted significantly higher by the contact cell co-culture compared to the pADSC, non-contact transwell and the SMC cultures respectively. Collagen 12a1 was secreted significantly higher by the contact cell co-culture compared to the SMC monoculture ($P^* < 0.01$), yet the pADSC expressed Col12a1 significantly higher than the contact co-culture ($P^* < 0.0001$). Fibronectin secretion was significantly increased in contact co-culture ($P^* < 0.01$) and the SMC monoculture ($P^* < 0.05$) compared to non-contact transwell co-culture and slightly decreased in the pADSC monoculture. The secretion of emilin1 was significantly higher in the contact co-culture compared to the non-contact transwell co-culture ($P^* < 0.01$) and the pADSC monoculture ($P^* < 0.05$), and was slightly decreased in the SMC monoculture. There was no significant difference between any of the samples in the secretion of Col8a2 (data not shown), while elastin was slightly increased in contact co-culture and Col15a1 was significantly higher deposited by pADSC compared to all other samples ($P^* < 0.0001$).

Proteomic analysis – ECM remodeling: In order to gain a better insight into the ECM remodeling, the secretion of matrix metalloproteinases (MMP) and tissue inhibitors of metalloproteinases (TIMP) by the cell co-cultures (contact and non-contact transwell co-cultures) was assessed (Fig. 6). Two groups with distinct patterns were identified within the seven detected MMP. Although there was no significant difference in the expression of MMP2, MMP14 and MMP23 between any of the samples, a distinct pattern was recognized. pADSC showed similar expression to contact co-culture, while the non-contact transwell co-culture showed the lowest secretion of all MMP. In the second group, pADSC exhibited a significantly higher secretion ($P^* < 0.01$) of MMP3, MMP9 and MMP13

compared to the contact and non-contact transwell co-cultures. Furthermore, the secretion of MMP19 by pADSC was significantly increased compared to all other conditions ($P^* < 0.01$). In addition, TIMP1, 2 and 3 were detected in the secretome of all samples. The secretion of TIMP1 by the contact co-culture was significantly higher compared to the non-contact transwell co-culture and the pADSC monoculture ($P^* < 0.01$). There was no significant difference in the secretion of TIMP2 and 3 between any of the samples, yet a similar pattern to MMP2, 14 and 23 was observed, indicating tight ECM remodeling. In order to further understand the cell-cell and cell-ECM interactions, integrin (Itg) expression in the respective cell pellets was assessed. Thereby, contact co-culture was compared to non-contact transwell pADSC and SMC co-cultures and to the respective monocultures (Fig. 7).

Proteomic analysis – Growth factors: A variety of growth factors involved in wound healing and tissue regeneration were found in the cell secretome (Fig. 8). Connective tissue growth factor (CTGF) secretion was significantly increased in the contact co-culture compared to the non-contact transwell co- ($P^* < 0.01$), the SMC ($P^* < 0.01$) and the pADSC monocultures ($P^* < 0.001$). Also, heparin-binding epidermal growth factor-like growth factor (HBEGF) was significantly higher secreted by the contact cell co-culture compared to the SMC monoculture ($P^* < 0.05$), with both other conditions showing slightly lower, yet not significantly different HBEGF secretion. Lastly, there was no significant difference in platelet-derived growth factor subunits (PDGF)-A and -D secretion between any of the samples. However, the contact cell co-culture showed an increased trend in PDGF secretion compared to all other conditions (Fig. 9 top). In addition, almost all members of the TGF- β family were detected in the secretome of all samples. Both, the contact and non-contact transwell co-cultures showed a significantly increased secretion of TGF- β 2 compared to both monocultures. There was no significant difference in the secretion of TGF- β 1 and TGF- β 3 between any of the samples, with the contact co-culture showing a slightly increased secretion of both growth factors compared to the SMC monoculture (Fig. 8 bottom).

Discussion

In this study, we investigated the differences between various SMC-pADSC co-cultures and compared them to the SMC monoculture in order to find a suitable cell ratio for future detrusor bioengineering. Our results show that the 1:1 cell ratio performs the closest to the SMC monoculture in terms of phenotype stability and contractility, while exhibiting an increased proliferation and organoid formation. Using a more pADSC-heavy cell ratio would be highly clinically desirable, yet such cell ratios yielded less promising results.

The characterization results confirmed that the SMC and pADSC used in this study expressed the specific bladder smooth muscle markers calponin and smoothelin in a similar manner as previously described in our laboratory [19]. The observed significantly decreased expression of the late myogenic differentiation marker MyH11 in pADSC compared to the SMC is likely due to the rather immature smooth muscle phenotype of the pADSC after three weeks of differentiation [30]. Yet, when combined with SMC in the 1:1 and 1:3 cell ratios, both cell types were morphologically indistinguishable from each other after one week of co-culture, evenly expressing the SMC specific markers at a similar level as the SMC control, indicating a further pADSC differentiation towards the SMC lineage [31]. In comparison, the 1:5 cell co-culture showed an uneven expression of the specific SMC markers even after two weeks of culture, which is likely due to the disparate SMC distribution in the predominant pADSC culture.

Besides affecting the pADSC phenotype, the SMC-pADSC ratio plays a significant role in the organoid formation and development over time, showing the highest number of organoids in the 1:1, followed by the 1:3 and 1:5 cell co-cultures and the SMC monoculture. As such, the SMC-based organoid formation may be of physiological origin and may well represent the formation of native bladder smooth muscle bundles in a 2D microenvironment [32]. When non-contact transwell co-cultured with pADSC, the SMC began to form organoids already after one week of culture. Thus, it seems that the organoid formation is accelerated upon the SMC-pADSC interaction and then progresses at a similar pace until the cell culture limits are reached.

In fact, the significant proliferation increase in the 1:1, 1:2 and 1:3 contact and non-contact transwell co-cultures further confirms a strong direct and paracrine interaction between

both cell types. Yet, in comparison, the 1:5 co-culture showed a significantly reduced proliferation and organoid formation. Hence, the observed beneficial effect is present only within a specific co-culture range and exceeding this cell ratio results in a limited synergistic effect. Based on our results, the pADSC layer surrounding the SMC organoid “core” in 2D and 3D co-culture shows strong similarities with a cell feeder layer and could be described as such[33].

The in-cell western blot analysis the 1:1 cell ratio shows an overall closest phenotype to the SMC monoculture. Interestingly, calponin shows a cell ratio-dependent expression decrease at the first week, while an equal α SMA and smoothelin expression decrease was observed at the two-week time point. Based on these results we hypothesize that a combination of these markers may be used to track smooth muscle maturation at an earlier (calponin) and a later stage (α SMA and smoothelin) of an SMC-pADSC co-culture.

The contractility test further confirmed the closest resemblance of the 1:1 cell co-culture to the SMC monoculture. Hence, the 1:1 cell ratio was chosen for the proteomic analysis. In order to understand the underlying mechanism of the organoid formation and assess the co-culture applicability for detrusor bioengineering, the focus of the proteomic analysis was set on ECM deposition and remodeling, integrin expression and growth factor secretion.

It has been shown previously that cultured SMC strongly express collagen type I, III, IV and fibronectin [34] and further exhibit a prominent collagen type III expression increase during strain [35]. Furthermore, it is known that the detrusor muscle is rich on collagen type I and III [36,37], and microfibrillar collagen type VI [38] and XII [39]. Also, bladder is rich on elastin, emilin and fibrillin fibers that recoil the bladder into their empty form after micturition [40]. Thus, our data showing a prominent expression of Col1a2, 2a1, 3a1, 6a2 and 12a1, as well as elastin, emilin1, fibrillin 1 are well in-line with the literature. Furthermore, the increased deposition of these ECM molecules in the 1:1 co-culture indicates a rapid formation of the SMC niche. We hypothesize that the increased deposition of the specific ECM molecules in the contact 1:1 co-culture is one of the major factors facilitating the organoid formation. In addition, a faster SMC niche generation may

also have caused the observed increase in cell proliferation of the SMC, while further strengthening the SMC phenotype in the pADSC during co-culture [41,42].

The very specific cellular organization within the organoids indicates a well-regulated cell-cell and cell-ECM interaction, remodeling and cell migration, which may in fact be a result of the various MMP detected in the cell secretome, out of which the MMP2 [43], 9 and 14 were previously identified in the bladder [40]. In addition, it has been shown that MMP2 and 9 expression is strain-dependent and leads to SMC migration and proliferation [35]. Interestingly, these MMP are also involved in neurite outgrowth, increased bioavailability of TGF β (MMP2), enhanced collagen affinity, collagen IV degradation (MMP2 and 9) and immunomodulation [44,45].

The secretion of TIMP1, 2 and 3 further indicates a tight control of the ECM deposition and remodeling. While TIMP1, which was slightly upregulated in the SMC and the 1:1 co-culture, heavily affects the activity of most of the detected MMP, including MMP2, 3, 9 and 13 [46], the weaker TIMP2 [47] additionally acts on MMP14 [48]. The usually ECM-bound TIMP3 [47] likely has a regulatory function in these processes as well, yet we assume it is comparably marginal as there does not seem to be any significant difference between the conditions.

In addition, the array of integrins found in the cell pellets play a crucial role in cell proliferation, differentiation, migration and functionality [49,50]. Particularly important for the cell-ECM interaction and cell motility are the RGD-binding α v β 3 and α 5 β 1, which were found to be highly overexpressed in the 1:1 co-culture, together with the laminin-binding, motility-related integrins α 1 β 1, α 2 β 1 and α 3 β 1 [40].

It is likely that the additional bulk of the detected ECM molecules and MMP were expressed as a reaction to the culture plate microenvironment, which is a common limitation of standard 2D culturing.

A variety of growth factors crucial for wound healing and detrusor formation were detected in the cell secretome, which may prove beneficial for a later detrusor bioengineering and regeneration *in vivo*. Interestingly, many of these factors were described to be essential in detrusor development and function as well as being

increasingly expressed upon mechanical strain in the detrusor muscle [51,52]. CTGF, which was highly overexpressed in the contact 1:1 co-culture has been shown to increase collagen mRNA and was described to be a marker of bladder wall remodeling after an outlet obstruction [53]. HBEGF, which was significantly increased in the contact co-culture has been shown to increase SMC mitogenicity[40], detrusor proliferation, hypertrophy and remodeling[35], indicating the involvement in the observed SMC proliferation increase and likely further facilitating the organoid formation. In addition, the detected PDGF family members A and D were described as potent mitogens and motility factors for SMC[54], and were shown to exhibit a pro-angiogenic function[55]. Furthermore, the detected members of the TGF- β family, mainly TGF- β 1 has been shown to be involved in detrusor organogenesis [52] and to promote stem cell differentiation into SMC [56], which may explain the observed, enhanced pADSC maturation towards the SMC lineage during co-culture.

These results may help to elucidate our findings, upon which the combination of SMC and pADSC in a 1:1 ratio improves the SMC proliferation, while further strengthening the SMC phenotype of the pADSC.

Conclusion

In conclusion, this study shows that SMC-pADSC co-culture in a 1:1 ratio may function as a replacement of the SMC monoculture to generate contractile smooth muscle tissue for detrusor muscle regenerative purposes. It offers a stable phenotype, improved proliferation, faster niche formation and increased secretion of various wound healing-related factors compared to the SMC monoculture.

Acknowledgements

We would like to thank Helmut Horten Foundation and Fromm Fellowship for their financial support that led to the completion of the study. In addition, we would like to thank the company Biognosys for performing the proteomic analysis at no charge and their subsequent support.

Disclosure Statement

None of the authors included in this manuscript have any financial or other conflicts of interest.

No competing financial interests exist.

Abbreviations

ADSC – adipose-derived stem cells

α SMA – alpha smooth muscle actin

BAM – bladder acellular matrix

BMP4 – bone morphogenetic protein 4

Col – collagen

CTGF – connective tissue growth factor

ECM – extracellular matrix

FBC – fetal bovine serum

HBEGF – heparin binding epidermal growth factor-like growth factor

HPRP - high-pH reverse phase chromatography

Itg - integrin

MMP – matrix metalloproteinase

MyH11 – myosin heavy chain 11

pADSC – pre-differentiated, smooth muscle-like adipose-derived stem cells

PBS – phosphate-buffered saline

PDGF – platelet-derived growth factor

PS – penicillin / streptomycin

SMC – smooth muscle cells

TGF- β – transforming growth factor-beta

TIMP – tissue inhibitor of metalloproteinases

References

- [1] Krstic R V. Human Microscopic Anatomy: An Atlas for Students of Medicine and Biology [Internet]. Springer Science & Business Media; 2013 [cited 2016 Feb 23]. Available from:
[https://books.google.ch/books?id=AMzsCAAQBAJ&lpg=PA336&dq=urinary bladder adventitia&hl=de&pg=PA336#v=onepage&q=urinary bladder adventitia&f=false](https://books.google.ch/books?id=AMzsCAAQBAJ&lpg=PA336&dq=urinary+bladder+adventitia&hl=de&pg=PA336#v=onepage&q=urinary+bladder+adventitia&f=false).
- [2] Deveaud CM, Macarak EJ, Kucich U, et al. Molecular analysis of collagens in bladder fibrosis. *J. Urol.* [Internet]. 1998 [cited 2018 Mar 23];160:1518–1527. Available from: [http://www.jurology.com/article/S0022-5347\(01\)62606-5/pdf](http://www.jurology.com/article/S0022-5347(01)62606-5/pdf).
- [3] Smolar J, Horst M, Sulser T, et al. Bladder regeneration through stem cell therapy [Internet]. *Expert Opin. Biol. Ther.* Taylor & Francis; 2018. p. 525–544. Available from: <https://www.tandfonline.com/doi/full/10.1080/14712598.2018.1439013>.
- [4] Ma F, Higashira H, Ukai Y, et al. A new enzymic method for the isolation and culture of human bladder body smooth muscle cells. *Neurourol Urodyn* [Internet]. 2002;21:71–79. Available from: <http://www.ncbi.nlm.nih.gov/pubmed/11835427>.
- [5] Huber A, Badylak SF. Phenotypic changes in cultured smooth muscle cells: limitation or opportunity for tissue engineering of hollow organs? *J Tissue Eng Regen Med* [Internet]. 2011/07/15. 2012;6:505–511. Available from: <http://www.ncbi.nlm.nih.gov/pubmed/21755602>.
- [6] Lin H-KK, Cowan R, Moore P, et al. Characterization of neuropathic bladder smooth muscle cells in culture. *J Urol* [Internet]. 2004/02/10. 2004 [cited 2016 Jun 20];171:1348–1352. Available from: <http://www.ncbi.nlm.nih.gov/pubmed/14767346>.
- [7] Dozmorov MGM, Kropp BBP, Hurst RRE, et al. Differentially expressed gene networks in cultured smooth muscle cells from normal and neuropathic bladder. *J. smooth muscle Res.* [Internet]. 2007 [cited 2014 Nov 3];43:55–72. Available from: <http://www.ncbi.nlm.nih.gov/pubmed/17598958>.

This paper has been peer-reviewed and accepted for publication, but has yet to undergo copyediting and proof correction. The final published version may differ from this proof.

Tissue Engineering

Pre-differentiated smooth muscle-like adipose-derived stem cells for bladder engineering (DOI: 10.1089/ten.TEA.2019.0216)

- [8] Sterodimas A, de Faria J, Nicaretta B, et al. Tissue engineering with adipose-derived stem cells (ADSCs): current and future applications. *J Plast Reconstr Aesthet Surg* [Internet]. 2009/12/09. 2010;63:1886–1892. Available from: http://www.ncbi.nlm.nih.gov/entrez/query.fcgi?cmd=Retrieve&db=PubMed&dopt=Citation&list_uids=19969517.
- [9] Zuk P, Zhu M, Ashjian P. Human adipose tissue is a source of multipotent stem cells. *Mol. Biol. ...* [Internet]. 2002 [cited 2014 Nov 6];13:4279–4295. Available from: <http://www.molbiolcell.org/content/13/12/4279.short>.
- [10] Zhu Y, Liu T, Song K, et al. Adipose-derived stem cell: A better stem cell than BMSC. *Cell Biochem. Funct.* [Internet]. 2008 [cited 2018 Feb 27];26:664–675. Available from: <http://www.ncbi.nlm.nih.gov/pubmed/18636461>.
- [11] Sgodda M, Aurich H, Kleist S, et al. Hepatocyte differentiation of mesenchymal stem cells from rat peritoneal adipose tissue in vitro and in vivo. *Exp. Cell Res.* [Internet]. 2007 [cited 2018 Feb 28];313:2875–2886. Available from: <http://www.ncbi.nlm.nih.gov/pubmed/17574236>.
- [12] Brzoska M, Geiger H, Gauer S, et al. Epithelial differentiation of human adipose tissue-derived adult stem cells. *Biochem. Biophys. Res. Commun.* [Internet]. 2005 [cited 2018 Feb 28];330:142–150. Available from: <http://www.ncbi.nlm.nih.gov/pubmed/15781243>.
- [13] Fujimura J, Ogawa R, Mizuno H, et al. Neural differentiation of adipose-derived stem cells isolated from GFP transgenic mice. *Biochem. Biophys. Res. Commun.* [Internet]. 2005 [cited 2018 Feb 28];333:116–121. Available from: <http://www.ncbi.nlm.nih.gov/pubmed/15939405>.
- [14] Fischer LJJ, McIlhenny S, Tulenko T, et al. Endothelial differentiation of adipose-derived stem cells: effects of endothelial cell growth supplement and shear force. *J. Surg. ...* [Internet]. 2009 [cited 2014 May 20];152:157–166. Available from: <http://www.sciencedirect.com/science/article/pii/S0022480408004332>.

- [15] Song YH, Shon SH, Shan M, et al. Adipose-derived stem cells increase angiogenesis through matrix metalloproteinase-dependent collagen remodeling. *Integr. Biol.* [Internet]. 2016 [cited 2018 Feb 28];8:205–215. Available from: <http://www.ncbi.nlm.nih.gov/pubmed/26758423>.
- [16] Rivera-Vald e S JJ, Garc a-Ba uelos J, Salazar-Montes A, et al. Human adipose derived stem cells regress fibrosis in a chronic renal fibrotic model induced by adenine. *PLoS One* [Internet]. 2017 [cited 2018 Feb 28];12:e0187907. Available from: <http://www.ncbi.nlm.nih.gov/pubmed/29281649>.
- [17] Leto Barone AA, Khalifian S, Lee WPA, et al. Immunomodulatory effects of adipose-derived stem cells: Fact or fiction? [Internet]. *Biomed Res. Int.* Hindawi Publishing Corporation; 2013 [cited 2018 Feb 28]. Available from: <http://dx.doi.org/10.1155/2013/383685>.
- [18] Rodr guez L V, Alfonso Z, Zhang R, et al. Clonogenic multipotent stem cells in human adipose tissue differentiate into functional smooth muscle cells. *Proc. Natl. Acad. Sci. U. S. A.* [Internet]. 2006 [cited 2017 Aug 17];103:12167–12172. Available from: <http://www.ncbi.nlm.nih.gov/pubmed/16880387>.
- [19] Salemi S, Tremp M, Plock JA, et al. Differentiated adipose-derived stem cells for bladder bioengineering. *Scand. J. Urol.* [Internet]. 2015;49:407–414. Available from: <http://informahealthcare.com/doi/abs/10.3109/21681805.2015.1004642>.
- [20] Wang C, Yin S, Cen L, et al. Differentiation of Adipose-Derived Stem Cells into Contractile Smooth Muscle Cells Induced by Transforming Growth Factor- β 1 and Bone Morphogenetic Protein-4. *Tissue Eng. Part A* [Internet]. 2010;16:1201–1213. Available from: <http://www.ncbi.nlm.nih.gov/pubmed/19895205>.
- [21] Ling Q, Wang T, Yu X, et al. UC-VEGF-SMC Three Dimensional (3D) Nano Scaffolds Exhibits Good Repair Function in Bladder Damage. *J. Biomed. Nanotechnol.* [Internet]. 2017 [cited 2017 Aug 22];13:313–323. Available from: <http://www.ingentaconnect.com/content/10.1166/jbn.2017.2343>.

This paper has been peer-reviewed and accepted for publication, but has yet to undergo copyediting and proof correction. The final published version may differ from this proof.

Tissue Engineering

Pre-differentiated smooth muscle-like adipose-derived stem cells for bladder engineering (DOI: 10.1089/ten.TEA.2019.0216)

- [22] Tremp M, Salemi S, Largo R, et al. Adipose-derived stem cells (ADSCs) and muscle precursor cells (MPCs) for the treatment of bladder voiding dysfunction. *World J Urol* [Internet]. 2014;32:1241–1248. Available from: <http://www.ncbi.nlm.nih.gov/pubmed/24217741>.
- [23] Zhu WD, Xu YM, Feng C, et al. Bladder reconstruction with adipose-derived stem cell-seeded bladder acellular matrix grafts improve morphology composition. *World J Urol* [Internet]. 2010;28:493–498. Available from: <http://www.ncbi.nlm.nih.gov/pubmed/20091038>.
- [24] Zhe Z, Jun D, Yang Z, et al. Bladder Acellular Matrix Grafts Seeded with Adipose-Derived Stem Cells and Incubated Intraperitoneally Promote the Regeneration of Bladder Smooth Muscle and Nerve in a Rat Model of Bladder Augmentation. *Stem Cells Dev* [Internet]. 2016;25:405–414. Available from: <http://www.ncbi.nlm.nih.gov/pubmed/26863067>.
- [25] Bunnell BA, Flaas M, Gagliardi C, et al. Adipose-derived stem cells: Isolation, expansion and differentiation. *Methods* [Internet]. 2008 [cited 2018 Mar 1];45:115–120. Available from: <https://www.sciencedirect.com/science/article/pii/S1046202308000601?via%3Dihub>.
- [26] Ngo P, Ramalingam P, Phillips JA, et al. Collagen gel contraction assay. *Methods Mol. Biol.* [Internet]. 2006 [cited 2018 Mar 6];341:103–109. Available from: <http://www.ncbi.nlm.nih.gov/pubmed/16799192>.
- [27] Bruderer R, Bernhardt OM, Gandhi T, et al. Optimization of Experimental Parameters in Data-Independent Mass Spectrometry Significantly Increases Depth and Reproducibility of Results. *Mol. Cell. Proteomics* [Internet]. 2017 [cited 2018 May 30];16:mcp.RA117.000314. Available from: <http://www.mcponline.org/lookup/doi/10.1074/mcp.RA117.000314>.

- [28] Hebert AS, Richards AL, Bailey DJ, et al. The One Hour Yeast Proteome. *Mol. Cell. Proteomics* [Internet]. 2014 [cited 2018 May 31];13:339–347. Available from: <http://www.mcponline.org/lookup/doi/10.1074/mcp.M113.034769>.
- [29] Kelstrup CD, Young C, Lavallee R, et al. Optimized fast and sensitive acquisition methods for shotgun proteomics on a quadrupole orbitrap mass spectrometer. *J. Proteome Res.* [Internet]. 2012 [cited 2018 May 31];11:3487–3497. Available from: <http://pubs.acs.org/doi/10.1021/pr3000249>.
- [30] Brun J, Lutz KA, Neumayer KMH, et al. Smooth Muscle-Like Cells Generated from Human Mesenchymal Stromal Cells Display Marker Gene Expression and Electrophysiological Competence Comparable to Bladder Smooth Muscle Cells. *Ro S*, editor. *PLoS One* [Internet]. 2015 [cited 2018 Jun 15];10:e0145153. Available from: <http://dx.plos.org/10.1371/journal.pone.0145153>.
- [31] Mvula B, Abrahamse H. Differentiation Potential of Adipose-Derived Stem Cells When Cocultured with Smooth Muscle Cells, and the Role of Low-Intensity Laser Irradiation. *Photomed. Laser Surg.* [Internet]. 2015;X:pho.2015.3978. Available from: <http://online.liebertpub.com/doi/10.1089/pho.2015.3978>.
- [32] Andersson K-EK, Arner A. Urinary bladder contraction and relaxation: physiology and pathophysiology. *Physiol. Rev.* [Internet]. 2004 [cited 2014 Nov 19];84:935–986. Available from: <http://www.physiology.org/doi/10.1152/physrev.00038.2003>.
- [33] Llames S, García-Pérez E, Meana Á, et al. Feeder Layer Cell Actions and Applications. *Tissue Eng. Part B Rev.* [Internet]. 2015 [cited 2018 Jun 18];21:345–353. Available from: <http://www.ncbi.nlm.nih.gov/pubmed/25659081>.
- [34] Baskin LS, Howard PS, Duckett JW, et al. Bladder smooth muscle cells in culture: I. Identification and characterization. *J. Urol.* [Internet]. 1993 [cited 2016 Feb 17];149:190–197. Available from: <http://www.ncbi.nlm.nih.gov/pubmed/8417209>.

- [35] Aitken KJ, Tolg C, Panchal T, et al. Mammalian target of rapamycin (mTOR) induces proliferation and de-differentiation responses to three coordinate pathophysiologic stimuli (mechanical strain, hypoxia, and extracellular matrix remodeling) in rat bladder smooth muscle. *Am. J. Pathol.* [Internet]. 2010 [cited 2018 Jun 21];176:304–319. Available from: <https://www.sciencedirect.com/science/article/pii/S0002944010603471?via%3Dihub>.
- [36] Longhurst PA, Eika B, Leggett RE, et al. Urinary bladder function in the tight-skin mouse. *J. Urol.* [Internet]. 1992 [cited 2018 Jun 21];148:1611–1614. Available from: <http://www.ncbi.nlm.nih.gov/pubmed/1433576>.
- [37] Chang SL, Howard PS, Koo HP, et al. Role of type III collagen in bladder filling. *Neurourol. Urodyn.* [Internet]. 1998 [cited 2018 Jun 21];17:135–145. Available from: <http://www.ncbi.nlm.nih.gov/pubmed/9514146>.
- [38] Brown AL, Brook-Allred TT, Waddell JE, et al. Bladder acellular matrix as a substrate for studying in vitro bladder smooth muscle-urothelial cell interactions. *Biomaterials* [Internet]. 2005 [cited 2014 May 15];26:529–543. Available from: <http://linkinghub.elsevier.com/retrieve/pii/S0142961204002042>.
- [39] Capolicchio G, Aitken KJ, Gu JX, et al. Extracellular matrix gene responses in a novel ex vivo model of bladder stretch injury. *J. Urol.* [Internet]. 2001 [cited 2018 Jun 21];165:2235–2240. Available from: <http://www.ncbi.nlm.nih.gov/pubmed/11371952>.
- [40] Aitken KJ, Bägli DJ. The bladder extracellular matrix. Part I: architecture, development and disease. *Nat. Rev. Urol.* [Internet]. 2009 [cited 2015 Dec 17];6:596–611. Available from: <http://www.ncbi.nlm.nih.gov/pubmed/19890339>.
- [41] Song Y, Song G. [Stem cell niche and its roles in proliferation and differentiation of stem cells]. *Sheng Wu Yi Xue Gong Cheng Xue Za Zhi* [Internet]. 2009 [cited 2018 Jul 17];26:195–198. Available from: <http://www.ncbi.nlm.nih.gov/pubmed/19334585>.

- [42] Gattazzo F, Urciuolo A, Bonaldo P. Extracellular matrix: A dynamic microenvironment for stem cell niche. *Biochim. Biophys. Acta - Gen. Subj.* 2014. p. 2506–2519.
- [43] Sutherland RS, Baskin LS, Elfman F, et al. The role of type IV collagenases in rat bladder development and obstruction. *Pediatr. Res.* [Internet]. 1997 [cited 2018 Jun 21];41:430–434. Available from: <http://www.nature.com/doi/10.1203/00006450-199703000-00021>.
- [44] Nagase H, Visse R, Murphy G. Structure and function of matrix metalloproteinases and TIMPs. *Cardiovasc. Res.* [Internet]. 2006 [cited 2014 Jul 15];69:562–573. Available from: <http://www.ncbi.nlm.nih.gov/pubmed/16405877>.
- [45] Rohani MG, Parks WC. Matrix remodeling by MMPs during wound repair. *Matrix Biol.* [Internet]. 2015;44–46:113–121. Available from: <http://linkinghub.elsevier.com/retrieve/pii/S0945053X15000530>.
- [46] Brew K, Nagase H. The tissue inhibitors of metalloproteinases (TIMPs): An ancient family with structural and functional diversity [Internet]. *Biochim. Biophys. Acta - Mol. Cell Res.* NIH Public Access; 2010 [cited 2018 Jul 20]. p. 55–71. Available from: <http://www.ncbi.nlm.nih.gov/pubmed/20080133>.
- [47] Masciantonio MG, Lee CKS, Arpino V, et al. The Balance Between Metalloproteinases and TIMPs: Critical Regulator of Microvascular Endothelial Cell Function in Health and Disease. *Prog. Mol. Biol. Transl. Sci.* [Internet]. Academic Press; 2017 [cited 2018 Jul 20]. p. 101–131. Available from: <https://www.sciencedirect.com/science/article/pii/S1877117317300121>.
- [48] Morgunova E, Tuuttila A, Bergmann U, et al. Structural insight into the complex formation of latent matrix metalloproteinase 2 with tissue inhibitor of metalloproteinase 2. *Proc. Natl. Acad. Sci.* [Internet]. 2002 [cited 2018 Jul 18];99:7414–7419. Available from: <http://www.ncbi.nlm.nih.gov/pubmed/12032297>.

- [49] Takada Y, Ye X, Simon S. The integrins. *Genome Biol.* 2007;8.
- [50] Danen EHJ. *Integrins: An Overview of Structural and Functional Aspects.* Austin (TX): Landes Bioscience; 2013.
- [51] Mirone V, Imbimbo C, Longo N, et al. The Detrusor Muscle: An Innocent Victim of Bladder Outlet Obstruction [Internet]. *Eur. Urol.* Elsevier; 2007 [cited 2018 Jul 2]. p. 57–66. Available from: <http://www.ncbi.nlm.nih.gov/pubmed/16979287>.
- [52] Islam SS, Mokhtari RB, Kumar S, et al. Spatio-Temporal Distribution of Smads and Role of Smads/TGF- β /BMP-4 in the Regulation of Mouse Bladder Organogenesis. *PLoS One.* 2013;8.
- [53] Chaqour B, Whitbeck C, Han J-S, et al. Cyr61 and CTGF are molecular markers of bladder wall remodeling after outlet obstruction. *Am. J. Physiol. Endocrinol. Metab.* [Internet]. 2002 [cited 2018 Jul 2];283:E765-74. Available from: <http://www.physiology.org/doi/10.1152/ajpendo.00131.2002>.
- [54] MacLellan DL, Steen H, Adam RM, et al. A quantitative proteomic analysis of growth factor-induced compositional changes in lipid rafts of human smooth muscle cells. *Proteomics* [Internet]. 2005 [cited 2018 Jun 22];5:4733–4742. Available from: <http://www.ncbi.nlm.nih.gov/pubmed/16267816>.
- [55] Justewicz DM, Shokes JE, Reavis B, et al. Characterization of the Human Smooth Muscle Cell Secretome for Regenerative Medicine. *Tissue Eng. Part C Methods* [Internet]. 2012 [cited 2018 Jun 22];18:797–816. Available from: <http://online.liebertpub.com/doi/abs/10.1089/ten.tec.2012.0054>.
- [56] Stowers RS, Drinnan CT, Chung E, et al. Mesenchymal stem cell response to TGF- β 1 in both 2D and 3D environments. *Biomater. Sci.* [Internet]. 2013 [cited 2018 Jun 15];1:860. Available from: <http://xlink.rsc.org/?DOI=c3bm60057b>.

Reprint Author:

Daniel Eberli, University Hospital Zürich, Frauenklinikstrasse 10, 8091 Zürich Switzerland.

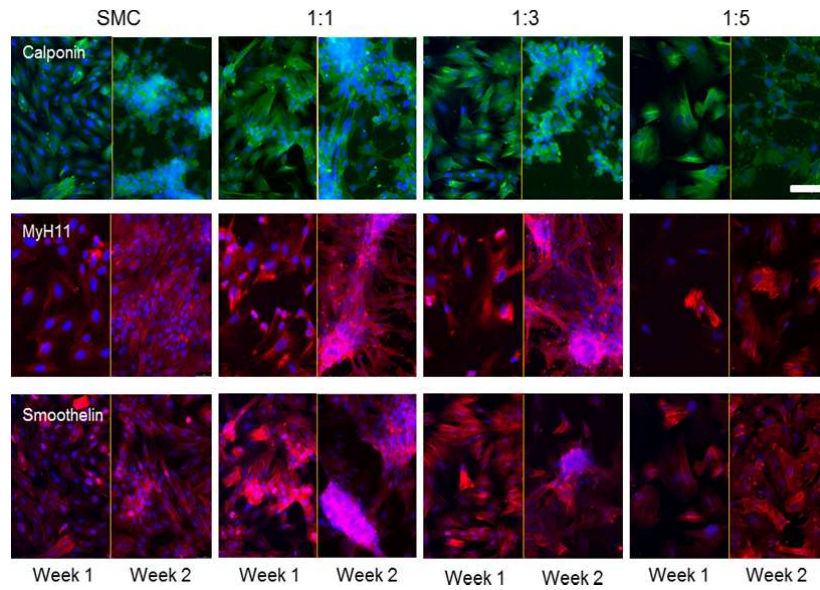


Figure 1: SMC marker expression by SMC and SMC-pADSC co-cultures in various ratios after one (left columns) and two weeks (right columns) of culture. The 1:1 and 1:3 ratios show a similar SMC marker expression to the SMC monoculture. The 1:5 cell ratio shows a weaker, rather inconsistent expression of the specific SMC markers. Calponin (green), MyH11 and Smoothelin (red). Nuclei (blue) stained with DAPI. Scale bar: 50 μ m

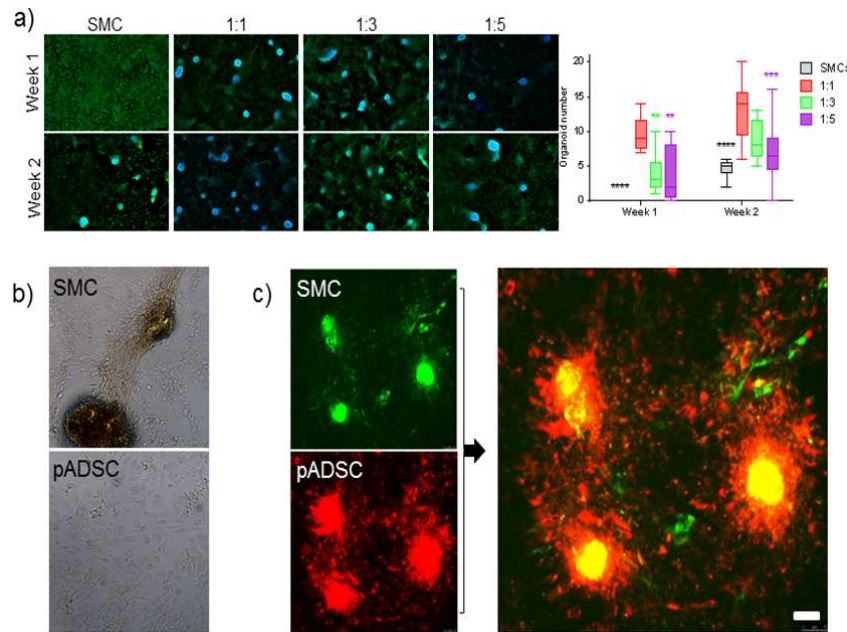


Figure 2: Organoid count and size in the co-cultures over three weeks of culture. The 1:1 cell ratio shows a significantly higher number of organoids compared to the other two cell ratios and the SMC monoculture after 1 and two weeks of culture. There was no significant difference in organoid size between the different cell ratios and the cell monoculture. Scale bar: 200 μ m b) SMC (top) after one week and pADSC (bottom) after three weeks of indirect cell co-culture in a 1:1 ratio. SMC do, while pADSC do not form organoids. c) SMC (top, green) and pADSC (bottom, red) were stained with pkh67 and pkh26 respectively and directly co-cultured for 2 weeks on glass chamber slides. SMC form the “core” of the organoid, while pADSC grow over and along the SMC as shown in the combined view. Scale bar: 75 μ m. **P<0.01, ***P<0.001, ****P<0.0001

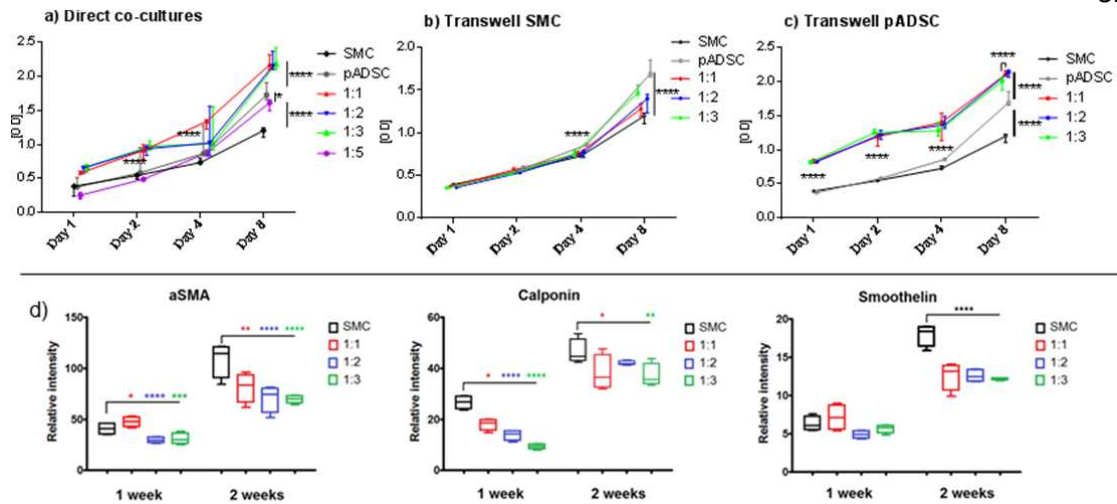


Figure 3: a) Proliferation analysis of cells grown by direct co-culture. In general the 1:1, 1:2 and 1:3 co-cultures proliferate significantly better than the monocultures. Cells in 1:5 ratio proliferate similarly to the pADSC monoculture. The 1:1 ratio shows the most continuous proliferation compared to other cell ratios.

b) Proliferation analysis of cells co-cultured using transwell inserts: SMC proliferation is significantly improved with the increasing number of pADSC. c) pADSC proliferate significantly faster when transwell co-cultured with SMC compared to the pADSC monoculture regardless the cell ratio. d) In-cell western blot analysis of cells grown in 96 well plates using the Li-COR system. In most cases the SMC marker expression in the 1:1 cell ratio is most similar to the SMC monoculture. * $P < 0.05$, ** $P < 0.01$, *** $P < 0.001$, **** $P < 0.0001$

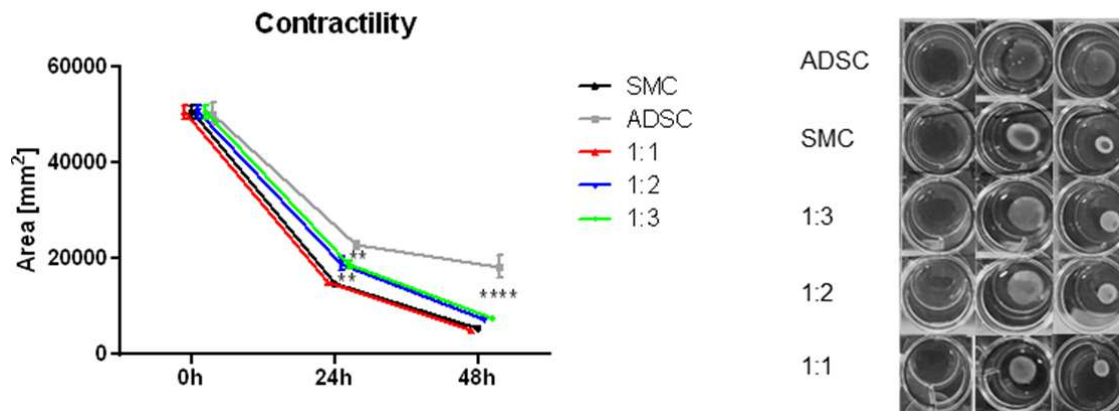


Figure 4: Contractility measurement of cells in various ratios embedded in collagen (contraction is marked by a red arrow). Cells in 1:1 ratio contract connatural to SMC monoculture. After 24h the 1:1 cell ratio shows a significantly improved functionality compared to other ratios, that normalizes after 48h. Overall co-cultures and SMC monoculture contract significantly better than the ADSC control. $****P<0.0001$

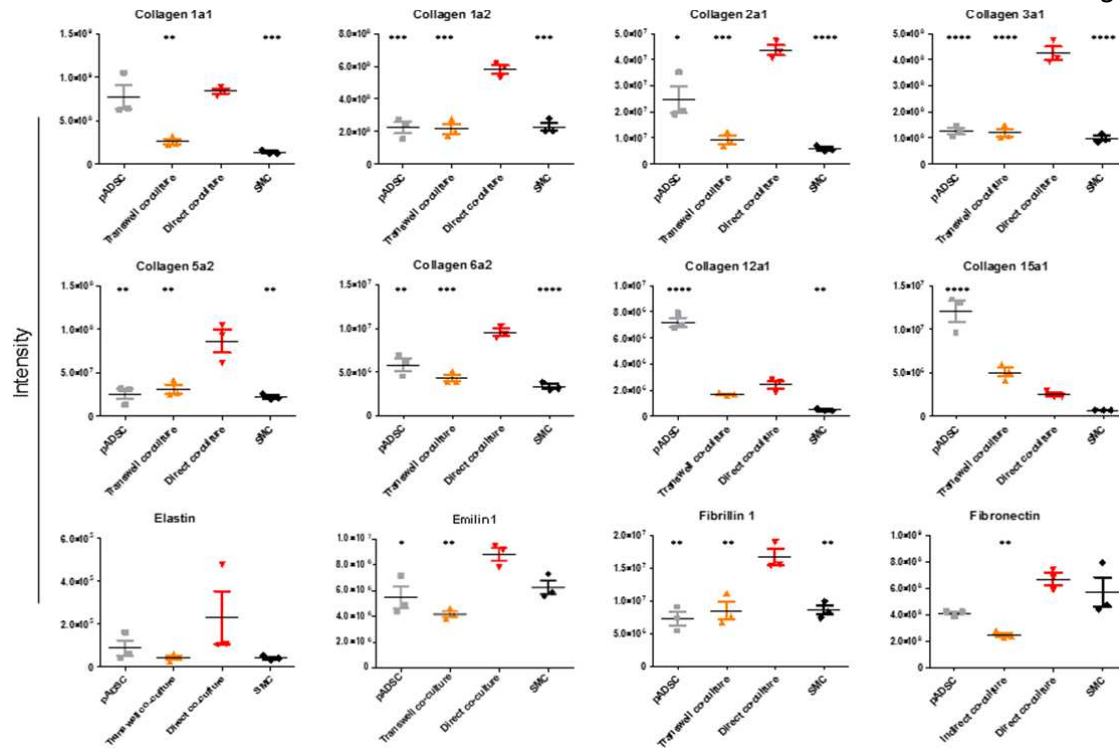


Figure 5: Proteomic analysis of the secreted ECM / niche proteins. *Significance was calculated in comparison to the 1:1 cell ratio using One-way ANOVA and a Bonferroni's multiple comparison test. Scatter dot plot \pm Min/Max; * $P < 0.05$, ** $P < 0.01$, *** $P < 0.001$, **** $P < 0.0001$*

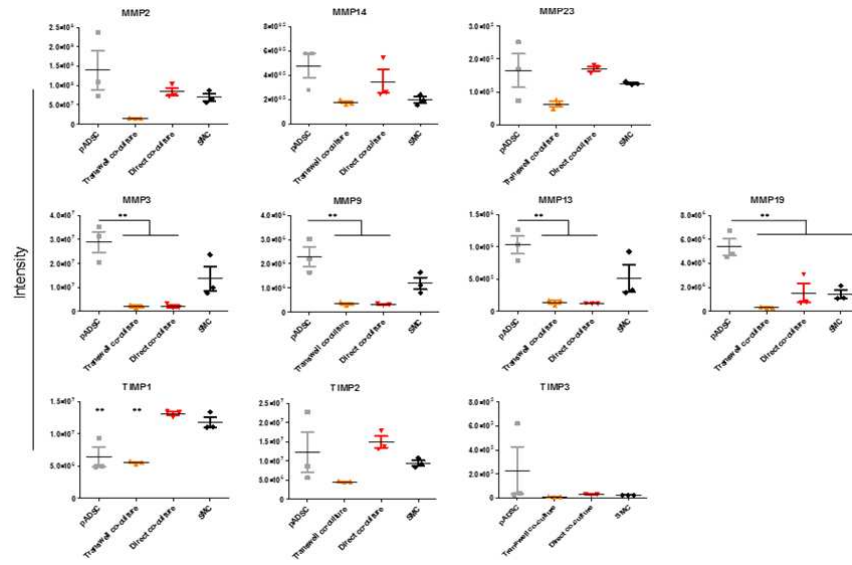


Figure 6: Proteomic analysis of the secreted MMPs and TIMPs. *Significance was calculated in comparison to the 1:1 cell ratio using One-way ANOVA and a Bonferroni's multiple comparison test. Scatter dot plot \pm Min/Max; **<0.01*

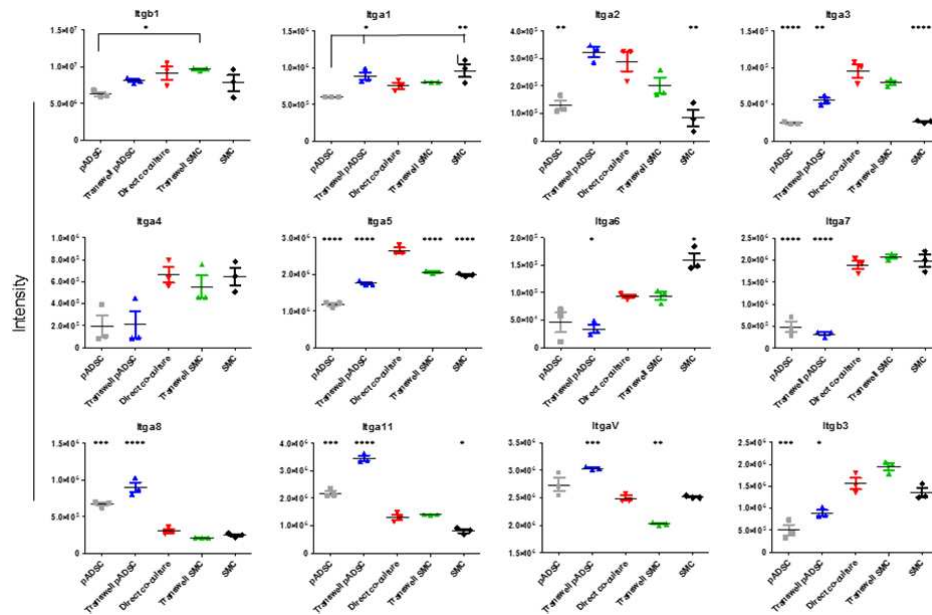


Figure 7: Proteomic analysis of the integrins. *Significance was calculated in comparison to the 1:1 cell ratio using One-way ANOVA and a Bonferroni's multiple comparison test. Scatter dot plot \pm Min/Max; * $P<0.05$, ** $P<0.01$, *** $P<0.001$, **** $P<0.0001$]*

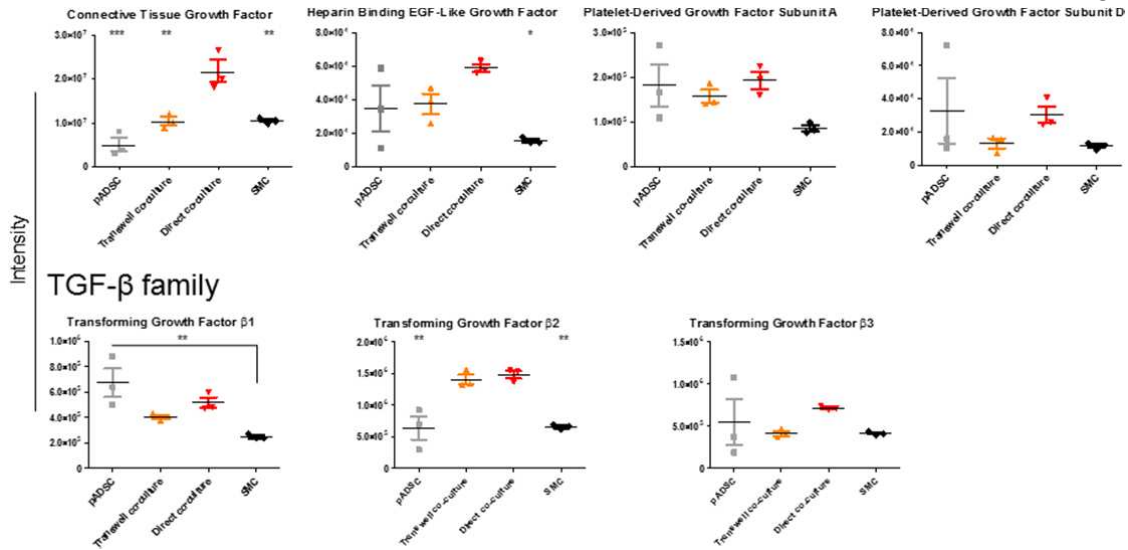
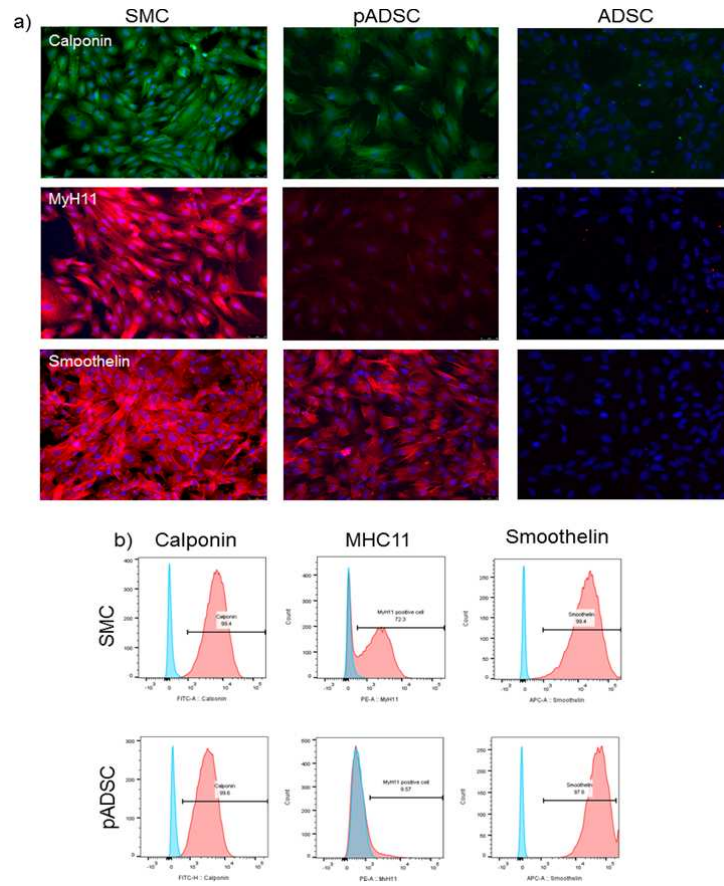
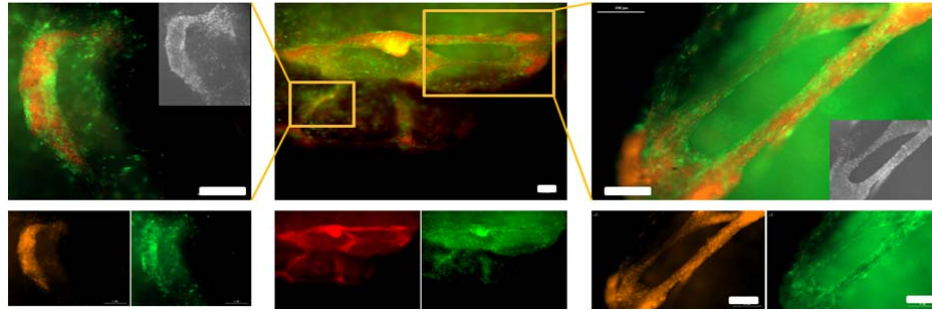


Figure 8: Proteomic analysis of various secreted growth factors and TGFβ isoforms. *9*Significance was calculated in comparison to the 1:1 cell ratio using One-way ANOVA and a Bonferroni's multiple comparison test. Scatter dot plot ± Min/Max; *P<0.05, **P<0.01, ***P<0.001

Figure Legends:



Suppl. Figure 1: a) Immunofluorescence staining of ADSC, pADSC and SMC for the expression of smooth muscle specific markers after one week of growth. ADSC did not express any of the specific markers. pADSC expressed calponin (green) and smoothelin (red) on a similar level as SMC, while their MyH11 (red) expression was decreased. b) representative SMC and pADSC flow cytometry analysis for the specific SMC markers after one week of culture in cell culture medium. Nuclei stained blue with DAPI.



Suppl. Figure. 2: SMC (red) and pADSC (green) after two weeks of direct co-culture in 1:1 ratio in collagen scaffold. SMC form organoids, networks and tubes in the scaffold that are surrounded by a pADSC layer. Grey pictures represent nuclei distribution in the organoids (DAPI staining). *Middle picture scale bar: 100µm, left and right pictures scale bars: 200µm*